Journal of Thermal Analysis and Calorimetry (2023) 148:10065–10079
https://doi.org/10.1007/s10973-023-12386-9

TG-MS study on the activity of Fe, Co, Ni, Cu, and Zn nanometal catalysts on thermal decomposition of ammonium perchlorate

Parvathy Chandrababu[1,2] · Sreeja Beena[3] · Deepthi Thomas[1] · Jayalatha Thankarajan[1] · Vishnu Sukumaran Nair[1] · Rajeev Raghavan[1]

Received: 3 November 2022 / Accepted: 12 July 2023 / Published online: 11 August 2023

Abstract

Five nanometal catalysts of Fe, Co, Ni, Cu and Zn were prepared by single displacement reaction and evaluated their catalytic activity towards thermal decomposition of ammonium perchlorate (AP) with respect to lowering of decomposition temperature, boosting of heat energy release and larger evolution of oxidizing decomposition products. The peak temperature of high temperature decomposition was decreased by 93, 55, 47, 15 and 13 °C by adding 0.5% each of Zn, Cu, Ni, Co and Fe respectively. The highest heat energy of 1910 J g^{-1} was obtained for 0.5% Cu. The evolved gases analysis using thermogravimetry-mass spectrometry revealed new inputs to the catalysed decomposition of AP, especially with respect to chlorine gas evolution. Among the five catalysts studied, copper nanometal powder emerged as the most promising catalyst for thermal decomposition of AP, which can improve the burn rate of the propellant enormously with reduced mass penalties.

Graphical abstract

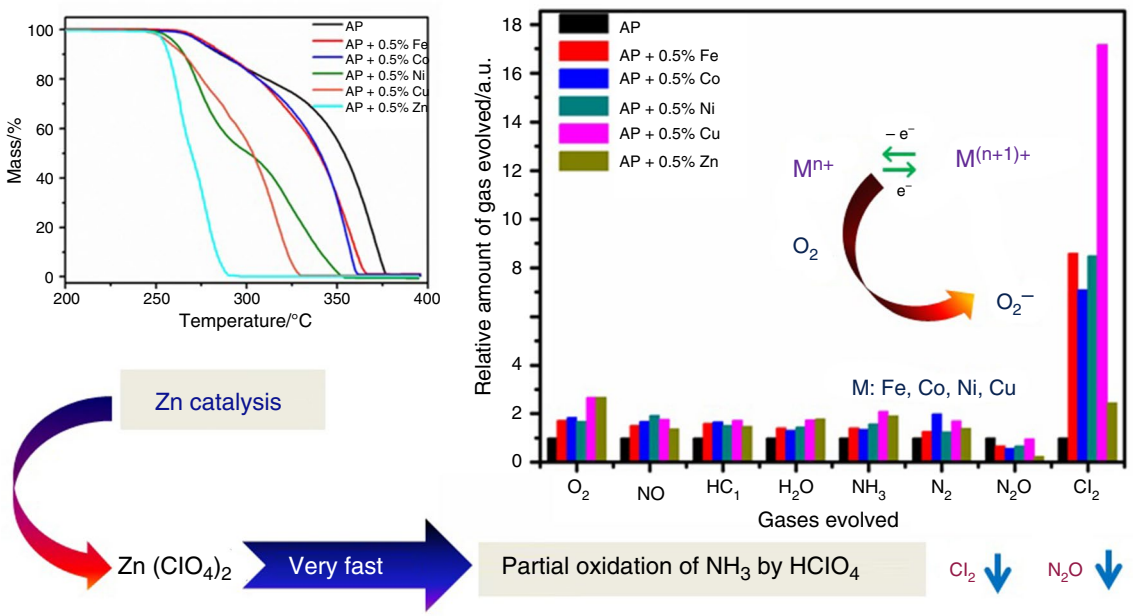

Keywords Transition metal catalysts · Single displacement reaction · Ammonium perchlorate · Thermal decomposition

Extended author information available on the last page of the article

Introduction

In aerospace and missile industry the key source of chemical energy for propulsion is composite solid propellants (CSPs), which is a heterogeneous mixture of a metallic fuel and an oxidizer embedded in a polymeric binder [1]. Ammonium perchlorate (AP) is an energetic material most commonly used oxidizer in CSPs [2] and being the major component (~ 70% of the propellant formulation) has crucial role in determining the burn rate of propellants. Nowadays, there is a great demand for high burn rate propellants having burn rate in the range of 20 to 25 mm s^{-1} for some specific applications viz., igniters, crew escape motors etc. By lowering the decomposition temperature of AP, the rate of combustion and burn rate of the propellant can be enhanced. This can be attained to some level by decreasing the particle size of AP. However, large variations in particle size affect the processability of the propellant adversely. Introduction of more energetic oxidisers or binders can improve the burn rates. However, these are highly sensitive, thermally unstable and mostly expensive and replacing the existing proven systems with such compounds require detailed chemical compatibility studies too [3, 4]. A third option is the incorporation of catalysts or burn rate modifiers, as thermal decomposition of AP is highly sensitive to presence of certain additives based on transition metal oxides. This has inspired many researchers to explore innovative burn rate modifiers for AP based propellants [5–7]. Nano sized transition metal oxides are known to be highly active catalyst for the thermal decomposition of AP compared to their microsized couter parts. The major characteristics of nanoparticles viz., ultrafine particle size and high surface area, can improve the catalytic activity of nanocatalysts to large extent. The nano sized transition metal oxides viz., CuO [8, 9], ZnO [10], Fe_2O_3 [11], NiO [2] and MnO_2 [12] are proven as effective catalysts for thermal decomposition of AP.

Recently transition metal nanoparticles have been reported as more active and efficient catalysts for the thermal decomposition reactions than their corresponding oxides. One of the reasons for this behaviour is that metals undergo oxidation with release of huge amount of heat during initial stages of the decomposition process, which can promote the rest of the decomposition reaction [13]. In addition, the in situ produced metal oxide catalysts are highly active than the synthesised and aged metal oxides. Duan et al. [14] investigated the catalytic effect of Ni nanoparticles on the thermal decomposition of AP and observed that addition of Ni nanoparticles (5 mass%) could decrease the decomposition temperature to a large extent (105 °C) and enhance the enthalpy change of decomposition by 796 J g^{-1}. Catalytic effect of nanometals viz., Ni, Cu and Al on thermal decomposition of AP was compared by Liu et al. They reported a reduction in the second stage decomposition of AP by 113, 130 and 52 °C in presence of 5 mass% of Ni, Cu and Al respectively [15]. Furthermore, supreme catalytic activity of nanometer sized metal catalysts over their micron sized ones was established in the study. Lan et al. [16] studied the effect of graphene/Ni aerogel nanoparticles prepared by sol–gel and supercritical carbon dioxide drying method on thermal decomposition of AP. 9 mass% of the nickel aerogel could decrease the decomposition temperature by 122 °C. Catalytic activity of Cu nanoparticles encapsulated with hexagonal boron nitride (h-BN) was investigated by Huang and team [17]. They could achieve an optimum balance between the high reactivity and stability of the nanoparticles by encapsulation of Cu nanoparticles with h-BN. Recently Rios et al. [18] reported the in situ preparation of copper nanoparticles supported on reduced graphene oxide using L-ascorbic acid as the reducing agent and its catalytic effect on thermal decomposition of AP. The presence of copper nanoparticles (3 mass%) as well as the supported system (1 mass%) could reduce the HTD of AP by 97 and 68 °C respectively. 49.9 °C decrease in decomposition temperature of AP could be achieved by Kechit and team by incorporating 1 mass% of iron-ionic liquid decorated multiwalled carbon nanotube [19].

Since the catalysts used for increasing the burn rate of propellants are considered as dead mass during propulsion, efforts are made to reduce the mass of catalyst by substituting more active or energetic catalyst in place of the currently used ones. Even though the catalytic effect of many materials has been a subject of research for the last decades, it is still a great challenge to find out newer catalysts with improved properties and minimum dead mass for space applications. This opens up new light in the area of catalytic thermal decomposition of AP with transition metal nanocatalysts. Even though the catalytic effect of some of the transition metals are reported as mentioned above, a detailed mechanism of transition metal catalysed thermal decomposition of AP is not much investigated. Reaction mechanism of AP still remains as vague, although lots of research works have already been carried out in this field [20, 21]. The reason is possibility of drawing thousands of reaction pathways considering all the oxidation states of all the four elements present in the simple molecule of AP. In addition, presence of chlorine makes AP different from most of the other propellants [13]. As thermal decomposition of AP follows a complex multi-step reaction pathway, attempts to unveil the process especially the catalyzed one even to some extent will be appreciated.

Exploding wire method [22], microwave reduction [23, 24], photochemical reduction [25], thermal reduction [26], chemical reduction [27–29], etc. are some of the synthesis routes

for preparation of nano sized metals. Among these, chemical reduction is comparatively convenient method as it is possible to tune the synthesis parameters (concentration, pH, reaction temperature) for moulding of metal nanoparticles with desired morphology, distribution and crystal structure, which has become highly critical for catalysis. Thus, the properties of the synthesised metallic particles can be engineered as per the requirement or application. Similar studies have been reported on synthesis of metal nanoparticles by chemical reduction using different reducing agents viz., hydrazine [30, 31], sodium borohydride [32], hydrazinium hydroxide [33], sodium hypophosphite [34], amines [35] etc. However, an environmentally benign synthesis needs some other reducing agent as all the above mentioned are harmful reagents. Recently Rios et al. reported synthesis of Cu nanoparticles using L-ascorbic acid, an environment friendly reducing agent [18].

In this paper we present a comparison of catalytic activity of transition metal nanocatalysts viz., Fe, Co, Ni, Cu and Zn on thermal decomposition pathways of AP emphasising the nature and amount the gaseous products evolved. The metals were selected for the study by expecting their supremacy over their oxides, proven catalysts for thermal decomposition of AP. For synthesis of the metallic catalysts, single displacement reaction using aluminium as reducing agent was opted as a simple, fast and efficient route. In this method, usage of the hazardous reducing agents could be avoided, making it an environmentally benign synthesis. The properties of the as-prepared catalysts were evaluated using various analytical techniques. Thermal analysis techniques viz., Thermogravimetry–Differential Scanning Calorimetry (TG-DSC) and Thermogravimetry- Mass Spectrometry (TG-MS) were employed for evaluation of kinetics and mechanism of the catalysed thermal decomposition of AP. TG-DSC, a simultaneous thermal analysis tool can provide information, regarding thermal stability, decomposition kinetics and enthalpy of decomposition with respect to temperature for both catalyzed and non-catalyzed reactions. Similarly, TG-MS is a hyphenated technique having combined capabilities of TG and MS for evolved gas analysis, which can be utilized as a potential tool for drawing new inputs on the mechanism of thermal decomposition of AP. Kinetic parameters are derived using non-isothermal Flynn/Wall/Ozawa (FWO) method. This is the work to date that investigates properties of the above mentioned transition metals prepared by single displacement reaction, compares their catalytic effect and derives a mechanism for transition metal catalyzed thermal decomposition reaction of AP.

Experimental

Materials

All the raw materials used for the present work viz., iron(III) chloride anhydrous ($FeCl_3$, 99.0%, Sisco Research Laboratories Pvt. Ltd., India), cobalt(II) chloride hexahydrate ($CoCl_2$. $6H_2O$, 99.0%, Merck Specialities Pvt. Ltd., India), nickel(II) chloride hexahydrate ($NiCl_2$. $6H_2O$, 99.0%, Merck Specialities Pvt. Ltd., India), copper (II) chloride dihydrate ($CuCl_2$. $2H_2O$, 99.0%, High purity laboratory chemicals, India), zinc chloride ($ZnCl_2$, 99.0%, Merck Specialities Pvt. Ltd.) and aluminium powder (99.0%, Merck Specialities Pvt. Ltd., India) were of analytical grade and used without further purification. 99% pure AP with average particle size of ≈ 50 µm, prepared in-house (by electrolytic oxidation of sodium chlorate followed by double displacement reaction with ammonium chloride) was used for the catalytic study. For preparation of solutions, distilled water was used.

Synthesis of transition metal catalysts

For the preparation of a transition metal catalyst (Fe, Co, Ni, Cu and Zn), 0.25 M solution of the corresponding precursor salt was prepared (100 mL) and was heated to 70 °C. To this solution about 0.45 g of aluminium powder (average particle size 15 µm) was added with constant stirring. The precipitated metallic powder was filtered, washed with water and dried at 110 °C for 30 min.

Instrumentation

X-ray powder diffraction (XRD) analysis was employed for phase identification of the prepared samples using Bruker D8 Discover diffractometer from 10 to 80° with Cu-Kα radiation (λ = 1.5406 A°) at a scanning rate of 4° min^{-1}. Surface morphology of the samples was captured using a Bruker Nano GmbH Gemini SEM 500 Field emission scanning electron microscope (FE-SEM). For a better understanding of reaction pathways of transition metal catalysed thermal decomposition of AP, evolved gas analysis by TG-MS was performed for pristine AP as well as AP-catalyst mix using Perkin Elmer Pyris 1 TGA Thermogravimetric analyser clubbed with a Perkin Elmer Clarus SQ8T Mass spectrometer.

Elemental analysis: The percentage of aluminium and other metallic impurities in each sample was measured using Perkin Elmer Optima 4300 V Inductively Coupled Plasma-Atomic Emission Spectrometer (ICP-AES). Metal content estimation in all the catalyst samples was performed

by titrimetric methods after digesting the metals in acid medium. The procedures are given below.

- Iron content: Iron content was determined by reducing ferric ion to ferrous ion using stannous chloride followed by titration against standard potassium dichromate using sodium diphenylamine as indicator.
- Cobalt, nickel and zinc content: The metal content was determined by treating the cobalt/ nickel/ zinc ions with excess EDTA in alkaline medium and titrating the unreacted EDTA against zinc sulphate solution using Eriochrome black T as the indicator.
- Copper content: Copper content was determined by iodometry using standard sodium thiosulphate as the titrant and starch as indicator.

Catalytic activity evaluation

Catalytic activity of synthesised transition metal catalysts on thermal decomposition of AP was evaluated using TG-DSC. For this, a mixture of AP with an average particle size of 50 µm and the nanometal catalyst in mass ratio 99.5:0.5 was thoroughly blended using an agate mortar and pestle. Approximately 5 mg of the mix was subjected to TG-DSC analysis by heating in a platinum pan under ultra pure nitrogen atmosphere at flow rate of 100 mL min^{-1} from room temperature to 400 °C at a heating rate of 5 °C min^{-1}. For DSC analysis an empty platinum pan was used as the reference. To check the homogeneity of the AP-catalyst mixture, mixing process was repeated two times and TG-DSC analyses were carried out for each mix.

Kinetic study

Thermal decomposition kinetics of AP with and without transition metal catalysts was carried out using FWO iso-conversional method [36–38]. Nonisothermal thermal decomposition of pristine AP and AP with metal catalyst at the three heating rates viz., 2, 5 and 10 °C min^{-1} was performed by TG analysis for the evaluation of the kinetic parameters viz., activation energy (E_a), pre-exponential factor (A) and rate constant (k).

FWO method: The activation energy, E_α at a constant conversion is determined using the Eq. 1.

$$E_\alpha = (\mathbf{R}/b)\triangle \mathbf{log}\beta/\triangle\left(\mathbf{1}/T_\alpha\right) \quad (1)$$

where, R is universal gas constant, β is heating rate in K min^{-1} and T_α is absolute temperature at constant conversion. $\Delta\log\beta/\Delta(1/T_\alpha)$ is the slope of the decomposition curves at different heating rates obtained by linear regression. Using Eq. 1, a first approximation of activation energy (E') is calculated from the slope of the curve with an initial b value of 0.457 K min^{-1}. Then second approximation of activation energy (E'') is calculated by using Doyle approximation value. The iterative process has been continued till a constant activation energy (E_α) is arrived. A series of E_α values are obtained with the conversion.

Equation 2 was used for calculating the Pre-exponential factor, A for the thermal decomposition reaction at each conversion and its average is reported.

$$\mathbf{A} = \left(-\beta\mathbf{R}/E_\alpha\right)[\mathbf{ln}(\mathbf{1}-a)]\mathbf{10}^{\mathrm{a}} \quad (2)$$

where, a is Doyle approximation value and α is fraction reacted (dimensionless).

From the average values of activation energy (E_a) and A, the rate constant, k of the reaction was calculated using the Arrehenius equation,

$$\mathbf{k} = \mathbf{A}\,\mathbf{e}^{(-\mathbf{Ea}/\mathbf{RT})} \quad (3)$$

Results and dicussion

Characterization of the transition metal catalysts

In order to understand the crystal structure of the as-prepared catalysts, XRD analysis was performed and presented in Figs. 1a–e. The XRD pattern (Fig. 1a) exhibits two peaks at 2θ of 44.68° and 65.12°, which is in accordance with the (110) and (200) planes of pure bcc Fe (0) crystals, respectively, according to JCPDS card no: 01–087-0721 [39]. The peaks located at 2θ of 41.84°, 44.38° and 47.77° in Fig. 1b are characteristic peaks assigned to the diffraction from the (100), (002) and (101) lattice planes for the hexagonal close packed cobalt (JCPDS card no. 05–0727) respectively [40]. The diffraction peaks at 44.54°, 51.91° and 76.53° in Fig. 1c coincide with (111), (200) and (220) of pure fcc Ni(0) respectively, as per standard PDF card (No. 04–0850) [41]. The XRD pattern of Cu (Fig. 5) contains the peaks characteristic of Cu_2O in addition to that of metallic Cu. All the diffraction peaks in Fig. 1d can be indexed based on the standard XRD data of metallic copper (PDF file no. 85–1326) [42] and Cu_2O (PDF file no. 77–0199) [43]. Here the peaks at 43.42°, 50.55° and 74.23° are arising from the (111), (200) and (220) planes of Cu and those at 29.71°, 36.54°, 42.44° and 61.49° are from (110), (111), (200) and (220) planes of Cu_2O respectively. Similarly X-ray diffractogram (Fig. 1e) of synthesized zinc also showed the presence trace amount of zinc oxide in it, in which the diffraction

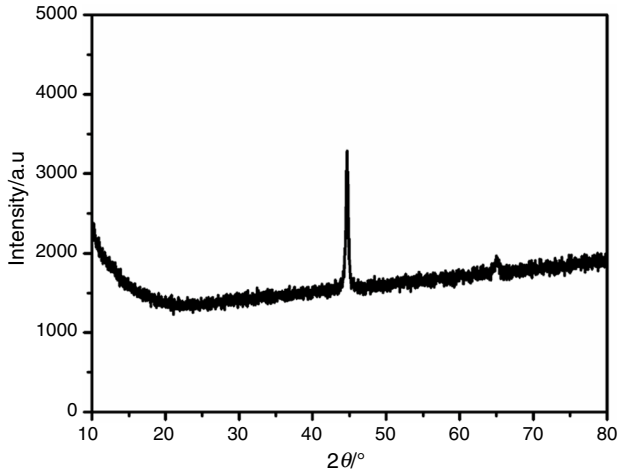

(a) XRD pattern of iron

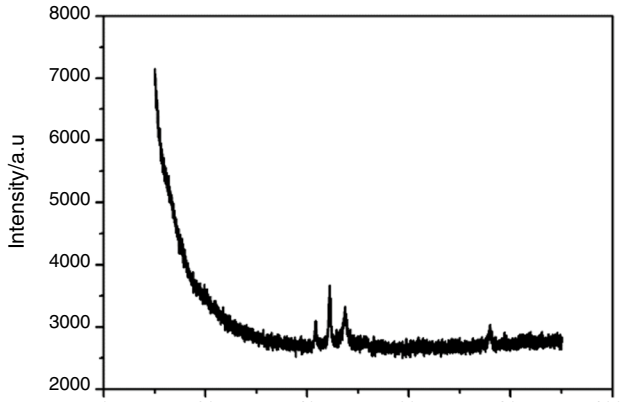

(b) XRD pattern of Cobalt

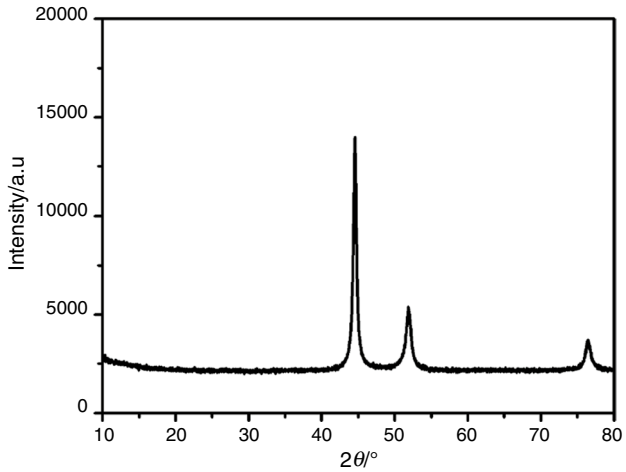

(c) XRD pattern of Nickel

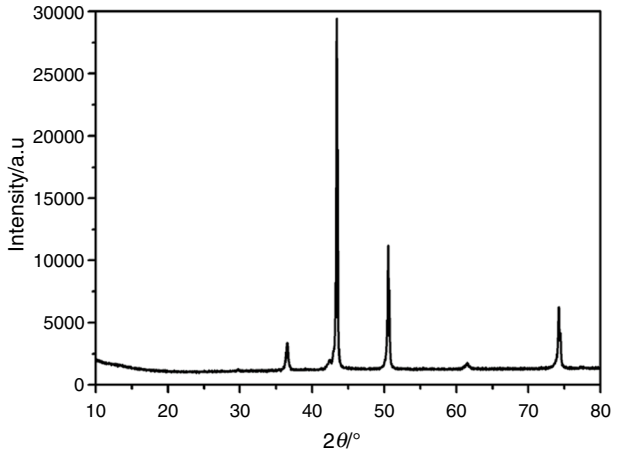

(d) XRD pattern of Copper

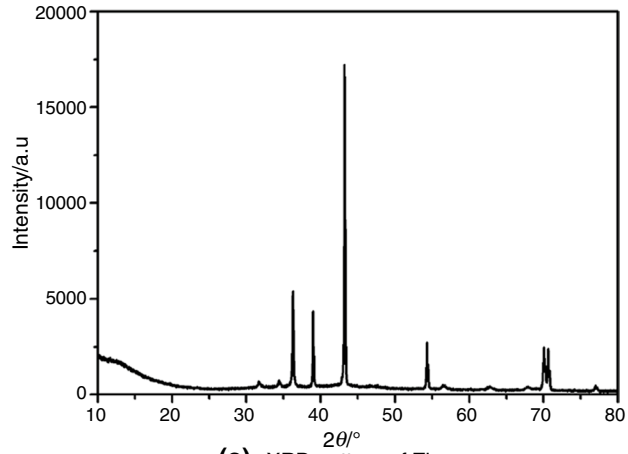

(e) XRD pattern of Zinc

Fig. 1 **a** XRD pattern of iron, **b** XRD pattern of cobalt, **c** XRD pattern of nickel, **d** XRD pattern of copper, **e** XRD pattern of zinc

Fig. 1 (continued)

peak at 36.21°, 38.94°, 43.17°, 54.27°, 70.06°, 70.70° and 76.99° can be attributed to diffraction from the (002), (100), (101), (102), (103), (110) and (004) planes of hexogaonal phase of metallic Zn (JCPDS card no. 03–065-5973) [44] and those at 31.71°, 34.47°, 56.48°, 62.73° can be attributed to diffraction from the (100), (002), (110) and (103) planes of hexagonal ZnO (JCPDS card no. 00–036-1451) [45]. Crystallite size of all the metals was calculated using Debye–Scherrer equation [46] and given in Table 1.

Assay calculated for all the as-prepared transition metal catalysts are given in Table 1, which reveals that the metals

Table 1 Properties of the as-prepared transition metal catalysts

Sample	Assay/%	Aluminium/%	Crystallite/nm
Iron	99.6	0.3	24
Cobalt	99.3	0.6	24
Nickel	98.0	1.9	18
Copper	98.7	0.2	77
Zinc	99.0	0.9	91

are of good purity. ICP-AES analysis was also performed for calculating any trace amount of aluminium present in the synthesized transition metals and the values obtained are given in Table 1. No other metallic impurities other than aluminium were detected in the five metal catalysts.

FE-SEM analysis was performed to understand the morphology of transition metals prepared by single displacement reaction and FE-SEM images captured are presented in Fig. 2a–e. From the FE-SEM analysis it is clear that the as-prepared metallic iron (Fig. 2a), cobalt (Fig. 2b) and nickel (Fig. 2c) consists of many nanoflakes, where cobalt exhibited flower like self-assembly of nanoflake like particles. FE-SEM image of copper catalyst (Fig. 2d) showed formation of cube shaped particles and that of zinc (Fig. 2) depicted the formation of mixed morphology consisting nanoflakes with nanoparticles crystallizing on its surface.

Thermal decomposition of AP

The kinetics and mechanism of thermal decomposition of AP are very sensitive to the presence of additives, otherwise known as burn rate modifiers or catalysts (e.g., transition metal or their oxides) and hence incorporation of such additives into AP accelerates its decomposition, which in turn can influence the ballistic performance of the AP containing propellants. A large number of research works have been carried out on thermal decomposition of AP and its reaction mechanism, but still, it is a subject of debate [47]. Pure AP undergoes two stage decomposition; low temperature decomposition (LTD, below 300 °C) corresponding to a mass loss of ~ 30% and high temperature decomposition (HTD, above 300 °C) which refers to the mass loss for the remaining 70% of the material. The major decomposition products formed during the decomposition reaction are HCl, NH_3, H_2O, O_2, NO, Cl_2, N_2, NO_2 etc. and the relative composition of the decomposition products and the decomposition temperature may vary with the presence of catalysts.

(a) FE-SEM image of Fe

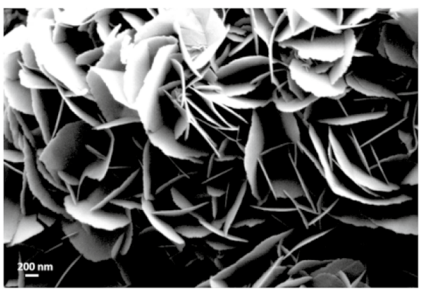

(b) FE-SEM image of Co

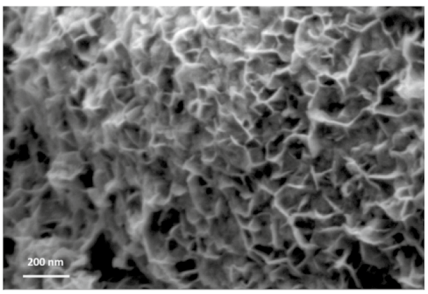

(c) FE-SEM image of Ni

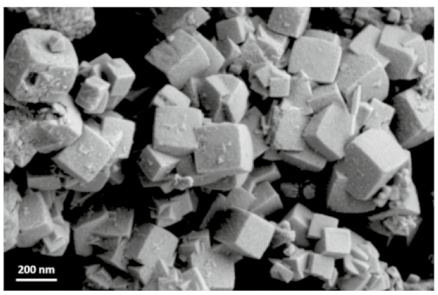

(d) FE-SEM image of Cu

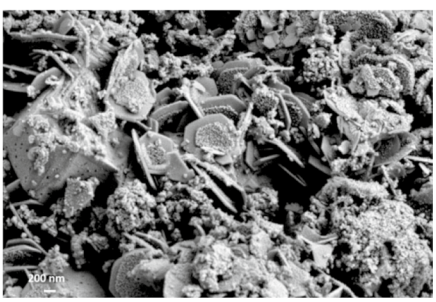

(e) FE-SEM image of Zn

Fig. 2 **a** FE-SEM image of Fe, **b** FE-SEM image of Co, **c** FE-SEM image of Ni, **d** FE-SEM image of Cu, **e** FE-SEM image of Zn

Among the different proposed mechanisms for the thermal decomposition of AP, the most accepted are electron transfer mechanism and proton transfer mechanism. According to electron transfer mechanism as proposed by Bircumshaw and Newman [48], the decomposition process proceeds via transfer of an electron from ClO_4^- anion to NH_4^+ cation, resulting in the formation of ClO_4^0 and NH_4^0 radicals.

$$NH_4ClO_4 \rightarrow NH_4^+ + ClO_4^- \rightarrow NH_4^0 + ClO_4^0 \quad (4)$$

As electron transfer occurs locally, the probability of its realisation is maximum when the distance between the ions is small. Hence the electron transfer occurs in ions present in interstitial spaces initially and mostly on the surface of the crystal. The ammonium radical formed immediately decomposes into ammonia and hydrogen.

$$NH_4^0 \rightarrow NH_3 + H \quad (5)$$

The resultant hydrogen migrates over the surface and interact with a ClO_4^0 radical to form perchloric acid, which again interacts with hydrogen and decompose into water and chlorate radical. Chlorate radical accept an electron and forms ClO_3^- and its further interaction of perchlorate radical, ammonium ion etc. results in the evolution of secondary products viz., Cl_2, nitrogen hemioxide and water.

$$ClO_4^0 + H \rightarrow HClO_4 \quad (6)$$

$$H + HClO_4 \rightarrow H_2O + ClO_3^0 \quad (7)$$

$$ClO_3 + 1\,e^- \rightarrow ClO_3^- \quad (8)$$

According to Boldyrev [49] ammonium perchlorate is a typical dielectric with a forbidden gap width of about 5.6 eV and hence the probability direct electron transfer is minimum especially at lower temperature.

In proton transfer mechanism proposed by Jacobs and Russel-Jones [50] decomposition or sublimation begins with transfer of proton from NH_4^+ ion to ClO_4^- anion held in an ion pair. A molecular complex is thus formed get decomposes into ammonia and perchloric acid.

$$NH_4^+ClO_4^- \rightleftarrows NH_3 - H - ClO_4 \rightleftarrows NH_3 - HClO_4 \rightleftarrows NH_3 + HClO_4 \quad (9)$$

These molecules react either on the surfaces of AP as in the adsorbed form or in the gas phase after getting desorbed and sublimed from the surface. The decomposition of $HClO_4$ molecules starts producing highly reactive oxidising species viz. ClO_3, ClO, Cl and O which exothermically react with ammonia to form H_2O, N_2O, NO, HCl, Cl_2, and N_2.

$$2HClO_4 \rightarrow ClO_3 + ClO + 3O + H_2O \quad (10)$$

$$2HClO_4 \rightarrow ClO_3 + ClO_2 + 2O + H_2O \quad (11)$$

$$2ClO \rightarrow O_2 + Cl_2 \quad (12)$$

$$2NH_3 + 4O \rightarrow N_2O + 3H_2O \quad (13)$$

$$NH_3 + 2O \rightarrow HNO + H_2O \quad (14)$$

$$ClO_2 + NH_3 \rightarrow N_2 + H_2O + Cl_2 \quad (15)$$

$$HClO_4 + HNO \rightarrow ClO_3 + NO + H_2O \quad (16)$$

Considering the physico-chemical changes happening during the process, the proton transfer mechanism was explained as [49], the reaction initiates with the formation of nuclei (the sites of defects or dislocations) as a result of proton transfer. This occurs in the pores at the subsurface level. Ammonia and perchloric acid formed during the proton transfer get separated in the pores due to the difference in diffusion rates. Accumulation of perchloric acid in the cavities cause drawing of proton by the neighbouring defects and also results in migration of the acid itself into neighbouring non-infected dislocations. The nuclei keep on growing to a size of 2–3 μm as the reactions proceed and stop growing when pressure inside the cavities increases to an order of 20 atm. Meanwhile, on the walls of the pores, perchloric acid decomposition products interact with unreacted AP. This causes increase in pore diameter and accumulation of water, which stabilize perchloric acid as well as chloric acid and there will be a cessation of LTD reaction as perchloric acid accumulation could not takes place in the pores with increased diameter. As the temperature increases (> 300 °C), the rate of desorption of adsorbed species on surface increases favouring the decomposition of AP to perchloric acid and oxidation of ammonia. Unlike LTD here the decomposition takes place mainly on surface of the crystal and hence will be temperature and pressure dependent. Secondary reactions involving decomposition of perchlorate and oxidation of ammonia occur either on the surfaces of AP as in the adsorbed form or in the gas phase after getting desorbed and sublimed from the surface.

In presence of catalysts the decomposition of AP becomes faster and the exothermicity of the reaction increases. The transition metals and their compounds especially oxides alter the course of the reaction by the lowering the decomposition temperature.

Literature clearly portrays that the catalysts have negligible influence on the initiation of the decomposition reaction. The catalysts mainly affect the electron transfer from Cl_4^- to NH_4^+ at low temperature and decomposition of $HClO_4$ by controlling the transformation of O_2 to superoxide ion

O_2^- at high temperature, which can further react with NH_3 to form N_2, NO and H_2O [51]**.** This reaction happens mainly on the surface of AP and hence a catalyst with high surface area and active sites can definitely catalyse the reaction. Therefore, the strong electron transfer property and high surface area of the catalyst have an important role on the thermal decomposition of AP.

In nutshell, both mechanisms indicate the formation of ammonia and perchloric acid for pure AP and it is assumed that low temperature conditions favour the proton transfer mechanism better than the electron transfer mechanism. In case of catalysesd thermal decomposition of AP, electron transfer mechanism dominates.

Variable oxidation states, small particle size, high surface area, defects and availability of acid sites make transition metal based compounds as potential catalysts for thermal decomposition reactions. Most of the catalysts like copper oxide, copper chromite, iron oxide, nickel oxide, etc. have no or very little impact on LTD of AP, but actively catalyse the HTD. Compounds like ZnO can affect both LTD and HTD [1, 6, 48]. As discussed earlier, transition metals are also known for excellent catalytic activity towards thermal decomposition of AP in comparison with the corresponding metal oxides and hence the effect of the synthesised transition metal powders on thermal decomposition of AP was subjected to detailed analysis using TG-DSC and TG-MS techniques.

TG-DSC analysis

The thermal decomposition of AP and AP with 0.5% of each of the catalysts was investigated with the help of simultaneous TG-DSC. From the overlaid TG-DTG curves of AP, AP + 0.5% Fe, AP + 0.5% Co, AP + 0.5% Ni, AP + 0.5% Cu and AP + 0.5% Zn shown respectively in Figs. 3a–f, it is clear that all the synthesized transition metals are having good catalytic effect. The phenomenological data of thermal decomposition of AP are tabulated and given in Table 2. Presence of 0.5% metal catalysts prepared via single displacement reaction could lower the decomposition temperature of AP and the effect was maximum for Zn catalyst and minimum for Fe catalyst. Among the five metal catalysts studied, Zn had maximum impact on LTD as well as HTD. The peak temperature (*Ts*) of LTD reduced by 12 °C in presence of 0.5% Zn catalysts. The peak temperature of HTD of AP decreased by 93, 55, 47, 15 and 13 °C for 0.5% each of Zn, Cu, Ni, Co and Fe respectively. The decrease in the decomposition temperature achieved in this paper is much better than the values reported earlier [9–12]. Thus the present work could showcase the advantage of well known single displacement reaction for the fast and facile synthesis of the transition metals with excellent catalytic activity via a green route (without using hazardous reducing agents). The

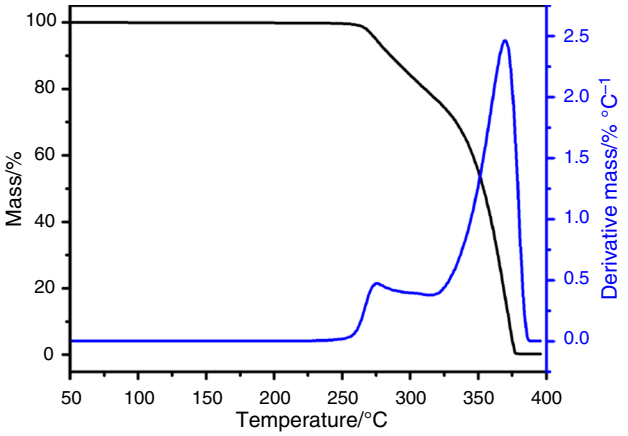

(a) Overlaid TG-DTG curve of AP

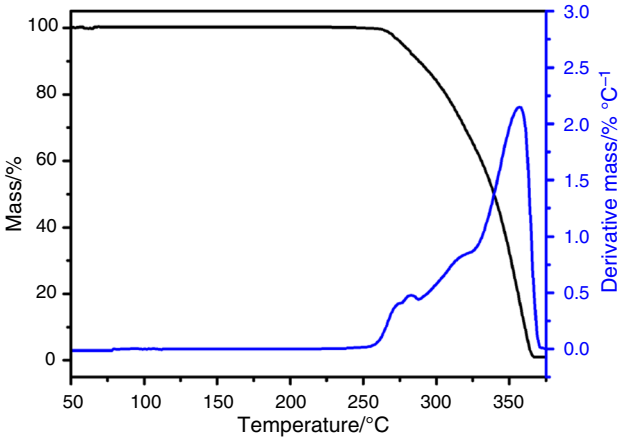

(b) Overlaid TG-DTG curve of AP with 0.5% Fe

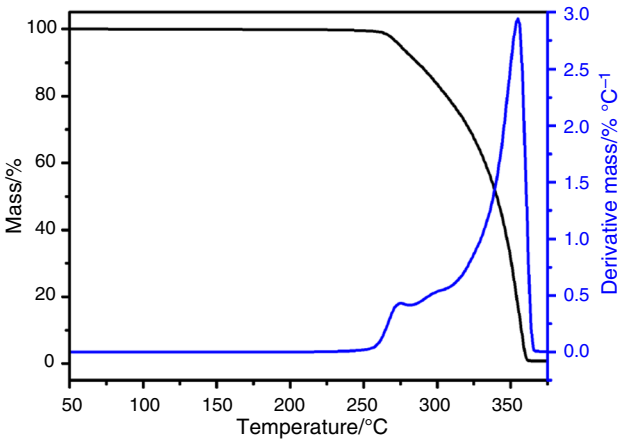

(c) Overlaid TG-DTG curve of AP with 0.5% Co

Fig. 3 **a** Overlaid TG-DTG curve of AP, **b** Overlaid TG-DTG curve of AP with 0.5% Fe, **c** Overlaid TG-DTG curve of AP with 0.5% Co, **d** Overlaid TG-DTG curve of AP with 0.5% Ni, **e** Overlaid TG-DTG curve of AP with 0.5% Cu, **f** Overlaid TG-DTG curve of AP with 0.5% Zn

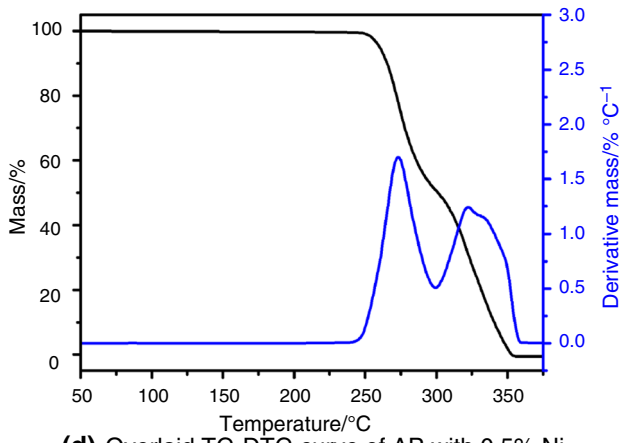

(d) Overlaid TG-DTG curve of AP with 0.5% Ni

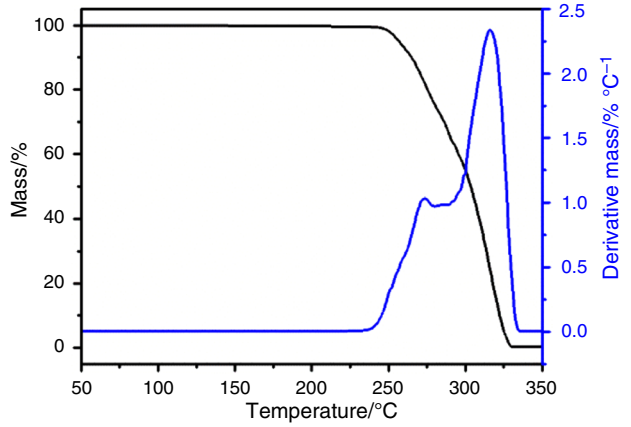

(e) Overlaid TG-DTG curve of AP with 0.5% Cu

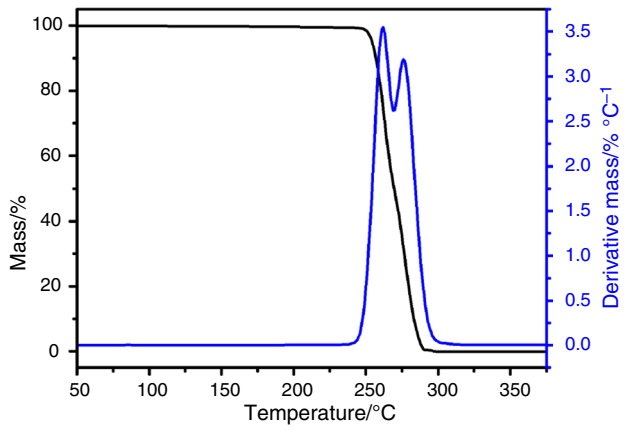

(f) Overlaid TG-DTG curve of AP with 0.5% Zn

Fig. 3 (continued)

trend observed in the catalytic activity can be attributed to their inherent chemical nature and is almost same as their oxides.

Figure 4 is the overlaid DSC curves of AP and AP with 0.5% transition metal catalysts viz., Fe, Co, Ni, Cu and Zn. The endothermic peak around 245 °C, which corresponds to the phase transition of AP from orthorhombic to cubic form, remain unaltered by the addition of the transition metal catalysts. As expected all the catalysts have impact on the enthalpy change (ΔH) of the decomposition reaction by making it more exothermic in nature, with the highest ΔH in presence of Cu (0.5 mass%). The increase in ΔH achieved in this study for 0.5% of Cu catalysts is ~ 1.2 times higher than the energy released for pure AP. The increased exothermicity of the catalysed reaction could trigger the combustion of AP containing propellant and thereby enhance the burn rate.

TG-DSC analysis revealed that Zn and Cu are having better activity as catalyst for the thermal decomposition of AP as compared to the other metallic catalysts viz., Fe, Co and Ni. In the transition metal catalysed thermal decomposition of AP, at first, the metals get converted to metal oxides by reacting with oxygen rich species released during the initial phase of the decomposition process. The in situ formed metal oxides are catalytically highly active due to their high surface area, low particle size and presence of large number of structural imperfections [13, 52]. These imperfections/defects in the metal oxides perform as active sites for the catalytic reaction. The extreme reduction in HTD observed in presence of Zn can be explained in terms of easy conversion of zinc oxide to zinc perchlorate, followed by its decomposition at very low temperature. Moreover, zinc perchlorate forms a eutectic with AP resulting in low temperature fusion, which further accelerates the reaction [53]. However, ΔH is not the highest for Zn catalysed reaction, which may be due to poor extent of reaction happening in presence of Zn with respect to Cu, which is further confirmed in the coming session, TG-MS analysis.

TG-MS study

Thermal decomposition mechanism of AP in presence of various transition metals was further investigated by evolved gas analysis using thermogravimetric analyser in combination with a mass spectrometer. Nature and relative abundance of gaseous products of thermal decomposition and the temperature at which gas evolution occurred were measured by this technique. Single ion chromatogram (SIC) for each volatile product were drawn using the data obtained from the TG-MS analysis of pure AP and AP mixed with transition metal catalysts (Fe, Co, Ni, Cu and Zn) and given in Fig. 5a–f. A bar chart showing the comparison of relative amount of each gas evolved during the thermal decomposition of AP with and without catalyst is given in Fig. 6.

TG-MS analysis of the decomposition of pure AP showed a two stage evolution of gaseous reaction products viz., Cl_2, N_2O, N_2, NH_3, H_2O, HCl, NO and O_2 with about 30% evolution during LTD and balance in HTD as depicted in Fig. 5a. For AP decomposition in presence of Cu and Zn, the two stages are almost merged together in the single ion

Table 2 Phenomenological data of TG/DTG/DSC analyses of AP with and without catalyst

Sample	First stage LTD/°C			Second stage HTD/°C			$\Delta H/J\ g^{-1}$
	T_i	T_s	T_f	T_i	T_s	T_f	
AP	248	275	315	315	370	388	1550
AP + 0.5% Fe	250	275	–	–	357	372	1700
AP + 0.5% Co	250	275	–	–	355	368	1740
AP + 0.5% Ni	244	273	300	300	323	360	1880
AP + 0.5% Cu	240	273	–	–	315	337	1910
AP + 0.5% Zn	242	263	270	270	277	304	1860

chromatograms while it is two stages for Fe, Co and Ni. In the case of Zn catalysed AP decomposition, the evolution gases during LTD is marginally higher than that during HTD while for all other cases evolution of gases during LTD is lower than that in HTD. In the case of zinc metal powder catalysed reaction, chlorine gas is evolved in a single stage while in all other cases two stage evolution of gases are observed. A number of intermediates especially oxides of chlorine are proposed to be formed during the course of the reaction but could not be detected by mass spectrometer due to the low stability of these species. These evolved gases supported the assumption that both LTD and HTD of AP follow the same type of reactions and produce similar products. The presence of ammonia in LTD and HTD stages indicates incomplete oxidation of ammonia by the perchlorate and its decomposition products which is often observed in fast gaseous reactions.

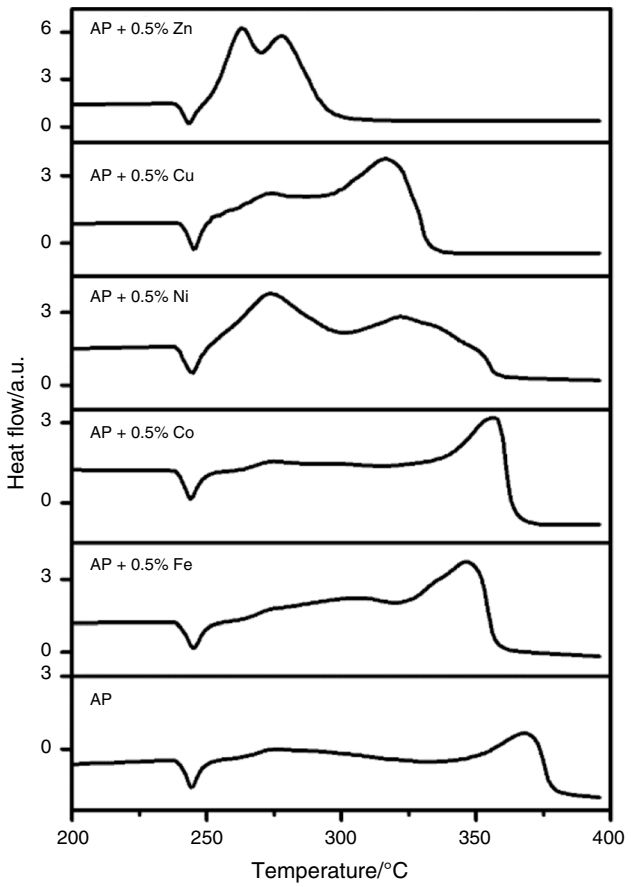

Fig. 4 Overlaid DSC curve of AP and AP with transition metal catalysts

All the five transition metal catalysts enhanced the reaction as reflected in the TG-DSC analysis, which is clear from the increase in the relative amount of gaseous products released for catalysed reaction rather than the non-catalysed one. The hike was observed for the all the gases in presence of catalysts except for N_2O. Ammonia release is higher in presence of Cu and Zn than that of Fe, Co and Ni. Nevertheless, there is a reduction in the relative amount of oxidation products of ammonia, particularly N_2O for Zn catalysed reaction as compared to Cu catalysed one. Another important observation from evolved gas analysis is huge difference in the relative amount of Cl_2 gas released during the catalysed decomposition of AP. However, the release of Cl_2 gas is comparatively less in presence of Zn. i.e., the extent of thermal decomposition reaction is less in presence of Zn leaving incomplete oxidation of ammonia and reduction in relative amount of Cl_2. The release of Cl_2 during the decomposition of AP is in the order AP–Cu > AP–Fe ≥ AP–Ni > AP–Co > AP–Zn > AP. Cl_2, O_2, and N_2O are considered as the secondary oxidising compounds released during the thermal decomposition of AP and release of large quantities of these gases will favour the oxidation of fuels present in AP containing propellant there by accelerating the combustion and burn rate of the propellant. Thus TG-MS analysis could clearly portray the superior catalytic proficiency Cu catalyst over the rest on thermal decomposition of AP. As the quantity of Cl_2 and N_2O released during Zn catalysed reaction is comparatively less, Zn may not be able to oxidise the fuels in a propellant effectively as the other transition metal catalysed systems.

TG-MS analysis supports electron transfer mechanism for the transition metal catalysed thermal decomposition of AP as their variable oxidation states and partially filled d-orbitals can enable them to act as good mediators for the process. Among the five metals studied, the higher conductivity and easily variable equilibrium of three oxidation

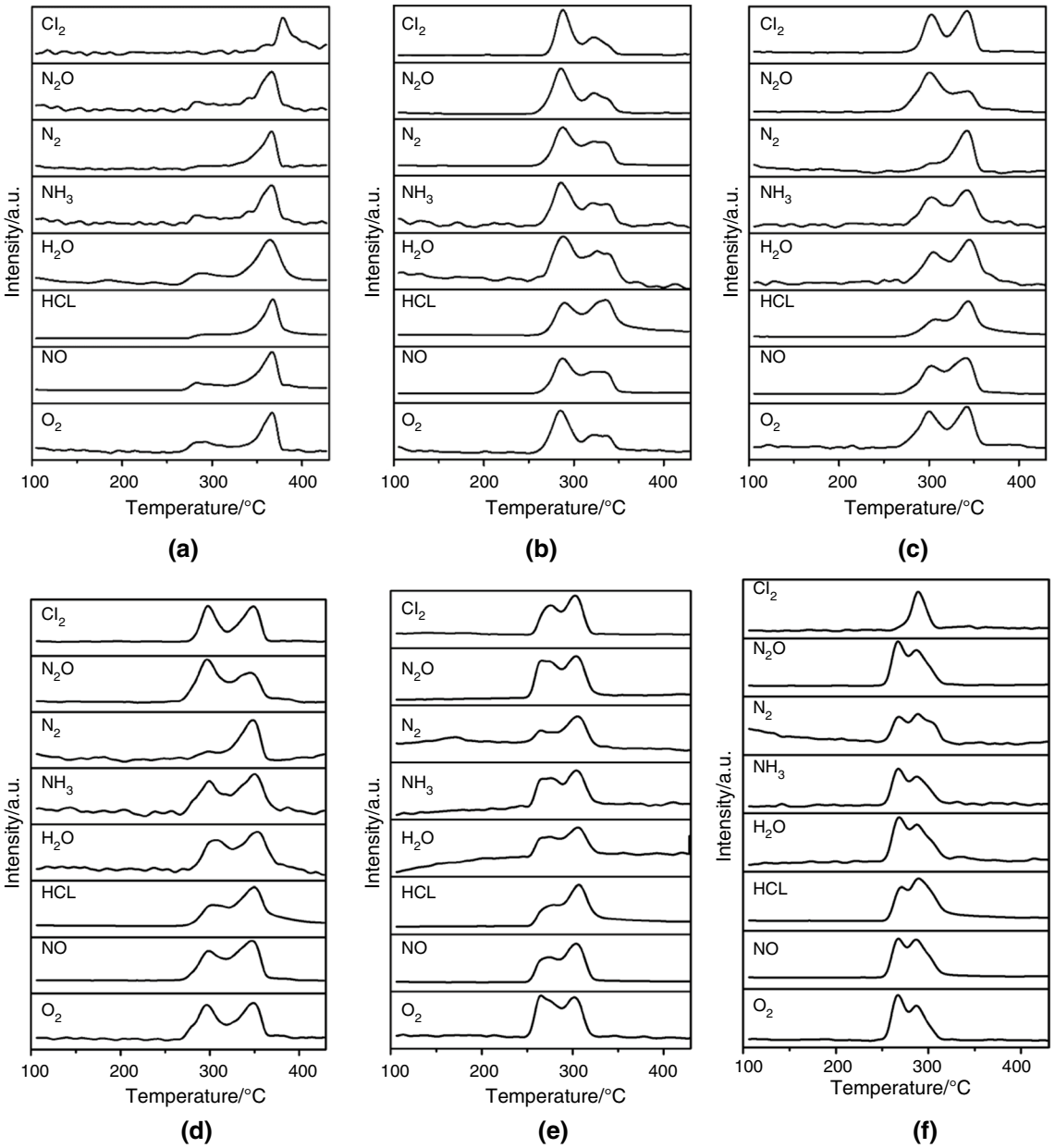

Fig. 5 SIC of **a.** AP, **b.** AP with 0.5% Fe, **c.** AP with 0.5% Co, **d.** AP with 0.5% Ni, **e.** AP with 0.5% Cu and **f.** AP with 0.5% Zn

states ($Cu \leftrightarrows Cu^{+} \leftrightarrows Cu^{2+}$) of Cu favours electron transfer mechanism for the decomposition of AP to greater extent. But Zn is an exception with completely filled d orbitals. In presence of Zn, the reaction proceeds via zinc perchlorate formation followed by its decomposition and eutectic formation with AP, which enhance the overall rate of the reaction profoundly. The very fast reaction ends up with incomplete thermal decomposition of AP resulting in partial oxidation of NH_3 and decrease in Cl_2 gas evolution. This poor extent of Zn catalysed reaction may be responsible for the lower ΔH value as observed in the TG-DSC analysis. Hence on the basis of electron transfer mechanism, the transition metal/oxides with partially filled d-orbitals and high conductivity for electrons are good catalysts for the thermal decomposition of $HClO_4$ and further oxidation of NH_3 molecules.

Thus both Cu and Zn are enhancing the thermal decomposition of AP but Cu is serving the real role as catalyst for thermal decomposition of the "propellant oxidizer ", AP with respect to lowering of decomposition temperature, boosting of heat energy release and larger evolution of oxidizing decomposition products. This supports electron transfer mechanism for the transition metal (except Zn) catalysed thermal decomposition of AP and the scheme of

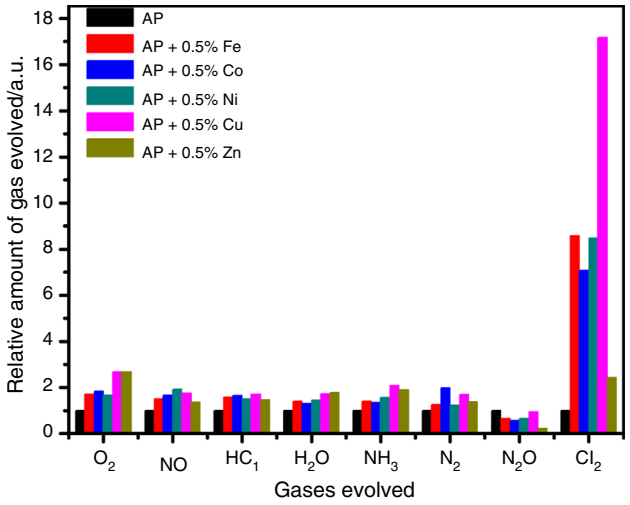

Fig. 6 Relative amount of gases evolved during the thermal decomposition of AP with and without catalysts

the reaction can be proposed as: Thermal decomposition of AP is having a self start ~ 260 °C irrespective of the catalyst. The oxidizing species evolved cause oxidation of the transition metal catalyst resulting in the formation of metal oxide. These metal oxides favours electron transfer process for rate controlling steps during the reaction via lower energy pathways by making the reaction faster. Thus transition metals enhance the electron transfer process to a greater extend by shifting the decomposition reaction to lower temperature with good energy release. Among the catalysts studied, Cu was proven as excellent catalyst for thermal decomposition of AP and good burn rate modifier for the propellant, as large quantities of the oxidizing species released can improve the combustion of the propellant.

Kinetic study

Among the five transition metal catalysts compared, Zn and Cu could accelerate the thermal decomposition of AP to higher degree. Hence for evaluation of the kinetic parameters viz., activation energy (E_a), pre-exponential factor (A) and rate constant (k), thermal decomposition of AP with and without catalyst (0.5 mass% each of Zn and Cu) were studied using FWO iso-conversional method. Figure 7a–c show the plots of linear relationship between logβ and $1000/T_\alpha$ for AP, AP with 0.5% Cu and AP with 0.5% Zn respectively and very good correlation between the two variables could be established at each conversion (5, 10, 20, 30, 40, 50, 60, 70, 80 and 90%). Using the Eqs. 1 and 2 and after incorporating Doyles approximation, activation energies and pre-exponential factors were calculated for each conversion.

AP decomposition being a complex reaction, the kinetic parameters thus determined at different conversion were

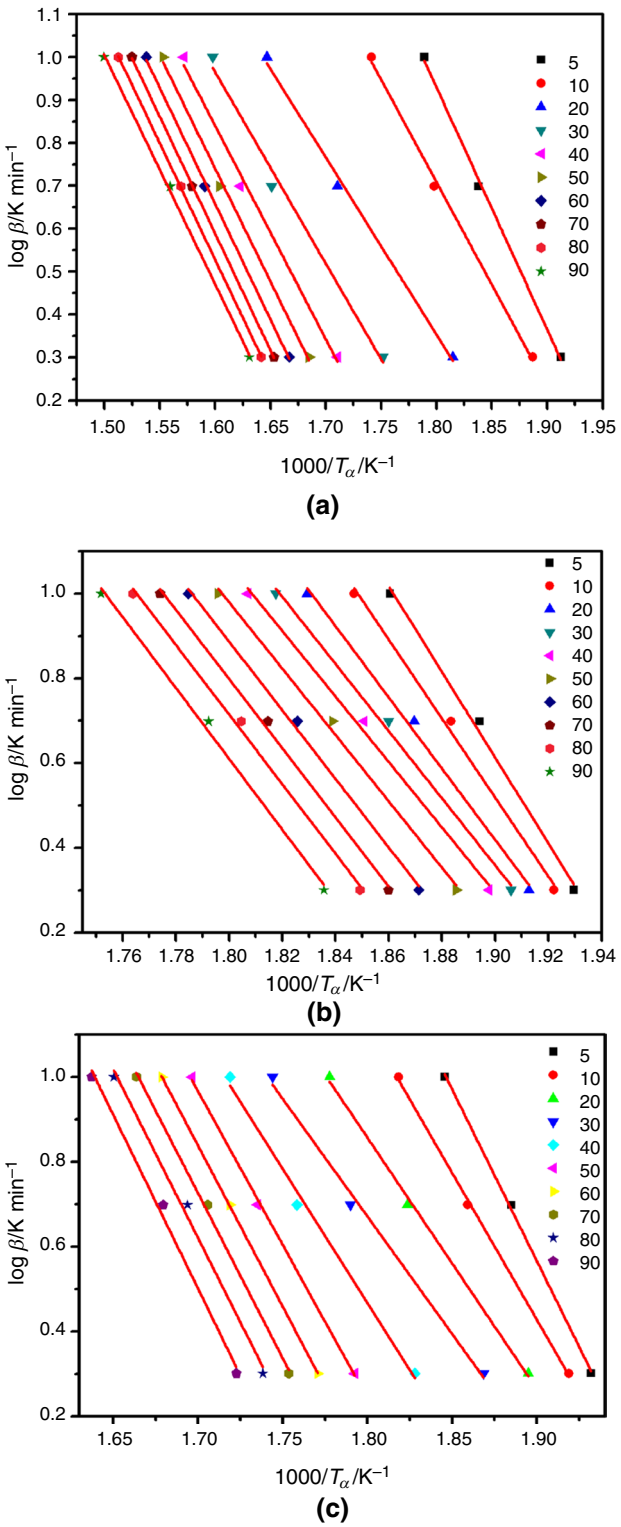

Fig. 7 Kinetics plots of AP decomposition using FWO method: **a**. pure AP, **b**. AP with 0.5% Zn and **c**. AP with 0.5% Cu

not similar as expected. The dependencies of activation energy on percentage conversion for AP and AP with catalysts determined by FWO method are depicted in Fig. 8.

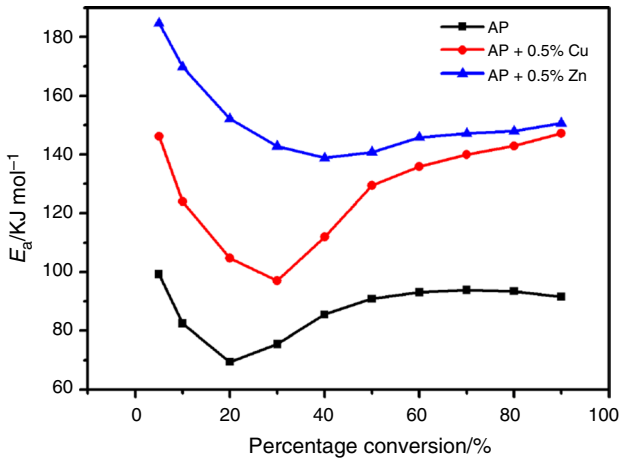

Fig. 8 Overlaid plots of dependency of activation energy with percentage conversion for AP and AP with catalysts

Table 3 Kinetic parameters for AP with and without catalysts

Sample	Avg. E_a/ kJmol^{-1}	Avg. A/min^{-1}	k/s^{-1}
AP	87	9.9×10^{6}	1.1×10^{-2}
AP + 0.5% Zn	152	3.9×10^{15}	2.4×10^{-1}
AP + 0.5% Cu	128	1.4×10^{12}	9.1×10^{-2}

The plot once again confirms the presence of two distinct stages of reaction for pristine AP and AP with 0.5 mass% of Cu catalyst as the activation energy values are reducing to 20–30% conversion followed by an increase. The pattern obtained in this study is similar to what reported for pure AP by Vyazovkin and Wight [54]. However, Zn catalysed reaction follows a different pattern as starting from higher values to lower ones and immediately attaining a plateau, which supports the disparate mechanism proposed via zinc perchlorate formation leading to incomplete reaction.

For further interpretation of the data, average values of activation energy (avg. E_a) and pre-exponential factor (avg. A) were calculated and applied in Arrhenius equation for deriving rate constant, k for AP with and without catalysts (given in Table 3), which is similar to some of the literature available. Domínguez calculated activation energies E_a for LTD and HTD as 87 and 198 kJ mol^{-1} for pristine AP, against 91 and 55 kJ mol^{-1} for AP with 5 mass% graphene [55]. Juibari and Eslami reported an increase in Ea from 115 to 140 kJ mol^{-1} for HTD of NiO catalysed thermal decomposition of AP [56]. Here also, it is to be noted that average activation energy as well as pre-exponential factor is increasing in presence of the catalysts. This may be due to kinetic compensation effect; the impact of a change in activation energy is compensated by an equivalent change in the pre-exponential factor [56–58].

The extreme catalytic activity of the as-synthesised Zn and Cu on thermal decomposition of AP was again confirmed by rate constant calculated using the Arrhenius equation. Approximately 22 times and 8 times hike in rate of the reaction could be achieved in the presence of 0.5 mass% Zn and Cu catalysts respectively.

Conclusions

In this work, transition metal catalysts viz., Fe, Co, Ni, Cu and Zn were synthesised by exploring single displacement reaction, as a fast, facile and environment benign method, for thermal decomposition of AP; their catalytic effect as well as mechanism of the decomposition reaction were compared. FE-SEM analysis depicted formation of nanoflakes of Fe, Co and Ni, cube shaped Cu nanoparticles and Zn as deposition of nanoparticles on nanoflakes. Elemental analysis proved that the as-prepared metals are of high purity. The peak temperature of HTD of AP decreased by 93, 55, 47, 15 and 13 °C for 0.5% each of Zn, Cu, Ni, Co and Fe respectively. The highest heat energy release was observed for 0.5% Cu catalyst, which was ~ 1.2 times higher than that of pure AP. The rate constant of thermal decomposition of the AP showed an increase from 1.1×10^{-2} s^{-1} to 2.4×10^{-1} s^{-1} and 9.1×10^{-2} s^{-1} in the presence of Zn and Cu respectively in the catalytic path. Evolved gas analysis by TG-MS study revealed the excellent catalytic activity of Cu on thermal decomposition of AP with the evolution of good amount of highly oxidizing species, especially chlorine. Thermal decomposition of AP in presence of Zn is 'incomplete' as it leads to partial oxidation of NH_3 and decrease in Cl_2 gas evolution. Hence the developed Cu metal is a promising catalyst for thermal decomposition of AP, which could improve the burn rate of the propellant enormously with reduced mass penalties.

Acknowledgements The authors acknowledge Director, VSSC, Deputy Director VSSC (PCM) and colleagues in Analytical and Spectroscopy Division, VSSC for their support.

Author contributions Conceptualisation, supervision and reviewing of the manuscript RR, Material preparation and data collection PC and SB, Data interpretation and manuscript preparation PC, Analysis DT, JT, VSN and PC.

Funding The authors have no relevant financial or non-financial interests to disclose.

Code availability Not applicable.

Declarations

Conflicts of interest Not applicable.

References

1. Jacob PWM, Whitehead HM. Decomposition and combustion of ammonium perchlorate. Chem Rev. 1969;69:551–90.
2. Wang Y, Zhu J, Yang X, Lu L, Wang X. Preparation of NiO nanoparticles and their catalytic activity in the thermal decomposition of ammonium perchlorate. Thermochim Acta. 2005;437:106–9.
3. Yan Q, Zhao F, Kuo KK, Zhang X, Zeman S, DeLuca LT. Catalytic effects of nano additives on decomposition and combustion of RDX-, HMX-, and AP-based energetic compositions. Prog Energy Combust Sci. 2016;57:75–62.
4. Bekhouche S, Trache D, Abdelaziz A, Tarchoun AF, Boukeciat H. Effect of fluorine-containing thermite coated with potassium perchlorate on the thermal decomposition behavior and kinetics of ammonium perchlorate. Thermochim Acta. 2022. https://doi.org/10.1016/j.tca.2022.179413.
5. Zhang J, Jin B, Hao W, Song Y, Hou C, Huang T, Peng R. Catalytic thermal decomposition of ammonium perchlorate by a series of lanthanide EMOFs. J Rare Earths. 2023;41:516–7.
6. Dave PN, Sirach R. $NiZnFe_2O_4$: a potential catalyst for the thermal decomposition of AP and burn rate modifier for AP/HTPB based propellants. J Therm Anal Calorim. 2022;147:10999–1012.
7. Chalghoum F, Trache D, Benziane M, Benhammada A. Effect of micro- and nano-CuO on the thermal decomposition kinetics of high-performance aluminized composite solid propellants containing complex metal hydrides. FirePhysChem. 2022;2:36–14.
8. Cui P, Wang A. Synthesis of CNTs/CuO and its catalytic performance on the thermal decomposition of ammonium perchlorate. J Saudi Chem Soc. 2016;20:343–8.
9. Benhammada A, Trache D, Chelouche S, Mezroua A. catalytic effect of green CuO nanoparticles on the thermal decomposition kinetics of ammonium perchlorate. Z fur Anorg Allg Chem. 2021;647:312–4.
10. Yang J, Zhang W, Liu Q, Sun W. Porous ZnO and ZnO–NiO composite nano/microspheres: synthesis, catalytic and biosensor properties. RSC Adv. 2014;4:51098–104.
11. Paulose S, Raghavan R, George BK. Graphite oxide–iron oxide nanocomposites as a new class of catalyst for the thermal decomposition of ammonium perchlorate. RSC Adv. 2016;6:45977–85.
12. Chen L, Zhu D. The particle dimension controlling synthesis of α-MnO_2 nanowires with enhanced catalytic activity on the thermal decomposition of ammonium perchlorate. Solid State Sci. 2014;27:69–72.
13. Chaturvedi S, Dave PN. A review on the use of nanometals as catalysts for the thermal decomposition of ammonium perchlorate. J Saudi Chem Soc. 2013;17:135–49.
14. Duan H, Lin X, Liu G, Xu L, Li F. Synthesis of Ni nanoparticles and their catalytic effect on the decomposition of ammonium perchlorate. J Mater Process Technol. 2008;208:494–8.
15. Liu L, Li F, Tan L, Ming L, Yi Y. Effects of nanometer Ni, Cu, Al and NiCu powders on the thermal decomposition of ammonium perchlorate. Propellants, Explos Pyrotech. 2004;29:34–8.
16. Lan Y, Jin B, Deng J, Luo Y. Graphene/nickel aerogel: an effective catalyst for the thermal decomposition of ammonium perchlorate. RSC Adv. 2016;6:82112–7.
17 Huang C, Liu Q, Fan W, Qiu X. Boron nitride encapsulated copper nanoparticles: a facile one-step synthesis and their effect on thermal decomposition of ammonium perchlorate. Sci Rep. 2015. https://doi.org/10.1038/srep16736.
18. Rios PL, Povea P, Cerda-Cavieres C, Arroyo JL, Morales-Verdejo C, Abarca G, Camarada MB. Novel *in situ* synthesis of copper nanoparticles supported on reduced graphene oxide and its application as a new catalyst for the decomposition of composite solid propellants. RSC Adv. 2019;9:8480–9.
19. Kechit H, Belkhiri S, Bhakta AK, Trache D, Mekhalif Z, Tarchoun AF. The effect of iron decorated MWCNTs and iron-ionic liquid decorated MWCNTs onto thermal decomposition of ammonium perchlorate. Z fur Anorg Allg Chem. 2021;647:1607–13.
20. Peiris SM, Pangilinan GI, Russell TP. Structural properties of ammonium perchlorate compressed to 5.6 GPa. J Phys Chem A. 2000;104:11188–6.
21. Xiao X, Peng B, Cai L, Zhang X, Liu S, Wang Y. The high efficient catalytic properties for thermal decomposition of ammonium perchlorate using mesoporous $ZnCo_2O_4$ rods synthesized by oxalate co-precipitation method. Sci Rep. 2018. https://doi.org/10.1038/s41598-018-26022-2.
22. Kadhem S, Humud H, Abdulmajeed IM. Copper nanoparticles prepared by pulsed exploding wire. Iraqi J Phys. 2015;13:128–38.
23. Sreeju N, Rufus A, Philip D. Microwave-assisted rapid synthesis of copper nanoparticles with exceptional stability and their multifaceted applications. J Mol Liq. 2016;221:1008–21.
24. Zhu H, Zhang C, Yin Y. Rapid synthesis of copper nanoparticles by sodium hypophosphite reduction in ethylene glycol under microwave irradiation. J Cryst Growth. 2004;270:722–8.
25. Giuffrida S, Condorelli GG, Costanzo LL, Fragala IL, Ventimiglia G, Vecchio G. Photochemical mechanism of the formation of nanometer-sized copper by UV irradiation of ethanol bis(2,4-pentandionato)copper(II) solutions. Chem Mater. 2004;16:1260–6.
26. Arul DN, Paul RC, Gedanken A. Synthesis, characterization, and properties of metallic copper nanoparticles. Chem Mater. 1998;10:1446–52.
27. Chakrapani V, Ahmed KBA, Kumar VV, Ganapathy V, Anthony SP, Anbazhagan V. A facile route to synthesize casein capped copper nanoparticles: an effective antibacterial agent and selective colorimetric sensor for mercury and tryptophan. RSC Adv. 2014;4:33215–21.
28. Nikhil VS, Thakare SR, Khaty NT. One pot synthesis of copper nanoparticles at room temperature and its catalytic activity. Arab J Chem. 2016;9:S1807–12.
29. Cerda JS, Gomez HE, A-Nunez G, Rivero IA, Ponce YG, Lopez LZF. A green synthesis of copper nanoparticles using native cyclodextrins as stabilizing agents. J Saudi Chem Soc. 2017;21:341–8.
30. Ong HR, Khan MR, Ramli R, Yunus RM. Synthesis of copper nanoparticles at room temperature using hydrazine in glycerol. Appl Mech Mater. 2014;481:21–6.
31. Nickel U, Castell A, Poppl K, Schneider S. A silver colloid produced by reduction with hydrazine as support for highly sensitive surface-enhanced raman spectroscopy. Langmuir. 2000;16:9087–91.
32. Lisiecki I, Billoudet F, Pileni MP. Control of the shape and the size of copper metallic particles. J Phys Chem. 1996;100:4160–6.
33. Wu SH, Chen DH. Synthesis of high-concentration Cu nanoparticles in aqueous CTAB solutions. J Colloid Interface Sci. 2004;273:165–9.
34. Tang XF, Yang ZG, Wang WJ. A simple way of preparing high-concentration and high-purity nano copper colloid for conductive ink in inkjet printing technology. Colloids Surf A: Physicochem Eng Asp. 2010;360:99–104.
35. Rice KP, Walker EJ, Stoykovich MP, Saunders AE. Solvent-dependent surface plasmon response and oxidation of copper nanocrystals. J Phys Chem C. 2011;115:1793–9.
36. ASTM Standard test method for decomposition kinetics by thermogravimetry using the Ozawa/Flynn/Wall method, designation: E1641–16.
37. Fynn JH, Wall LA. General treatment of the thermogravimetry of polymers. J Res Nat Bur Standards Part A. 1966;70A(5):487–523.
38. Vyazovkin S, Burnham AK, Criado JM, Pe´rez-Maqueda LA, Popescu C, Sbirrazzuoli N. ICTAC kinetics committee

recommendations for performing kinetic computations on thermal analysis data. Thermochim Acta. 2011;520:1–19.
39. Hirano Y, Kasai Y, Sagata K, Kita Y. Unique approach for transforming glucose to c3 platform chemicals using metallic iron and a Pd/C catalyst in water. Bull Chem Soc Jpn. 2016;89:1026–33.
40. Li CC, Zeng HC. Cobalt (hcp) nanofibers with pine-tree-leaf hierarchical superstructures. J Mater Chem. 2010;20:9187–92.
41. Wu X, Xing W, Zhang L, Zhuo S, Zhou J, Wang G, Qiao S. Nickel nanoparticles prepared by hydrazine hydrate reduction and their application in supercapacitor. Powder Technol. 2012;224:162–7.
42. Andal V, Buvaneswari G. Effect of reducing agents in the conversion of Cu_2O nanocolloid to Cu nanocolloid. Eng Sci Technol Int J. 2017;20:340–4.
43. Huang C, Long Z, Miyauchi M, Qiu X. A facile one-pot synthesis of Cu–Cu_2O concave cube hybrid architectures. Cryst Eng Comm. 2014;16:4967–72.
44. Mai NT, Thuy TT, Mott DM, Maenosono S. Chemical synthesis of blue-emitting metallic zinc nano-hexagons. Cryst Eng Comm. 2013;15:6606–10.
45. Billeh BM, Naciri AE, Moadhen A, Rinnert H, Guendouz M, Battie Y, Chaillou A, Zaibi MA, Oueslati M. Effects of silicon porosity on physical properties of ZnO films. Mater Chem Phys. 2016;175:233–40.
46. Usman MS, Ibrahim NA, Shameli K, Zainuddin N, Yunus WMZW. Copper nanoparticles mediated by chitosan: Synthesis and characterization via chemical methods. Molecules. 2012;17:14928–36.
47. Herve R, Li N, Geng Z, Cao M, Ren L, Zhao X, Liu B, Tian Y, Hu C. Well-dispersed ultrafine Mn_3O_4 nanoparticles on graphene as a promising catalyst for the thermal decomposition of ammonium perchlorate. Carbon. 2013;54:124–32.
48. Bircomshaw LL, Newman BH. Thermal decomposition of ammonium perchlorate. II. The kinetics of the decomposition, the effect of particle size and discussion of results. Proc Roy Soc A. 1955;227:228–41.
49. Boldyrev VV. Thermal decomposition of Ammonium perchlorate. Thermochim Acta. 2006;443:1–36.
50 Jacobs PWM, Russell-Jones. On the mechanism of the decomposition of ammonium Perchlorate. AIAA J. 1967;5:829–30.
51. Wang J, Zhang W, Zheng Z, Gao Y, Ma K, Ye J, Yang Y. Enhanced thermal decomposition properties of ammonium perchlorate through addition of 3DOM core-shell Fe_2O_3/Co_3O_4 composite. J Alloys Compds. 2017;724:720–7.
52. Wang T, Xu B, Wang Y, Lei J, Qin W, Gui K, Ouyang C, Chen K, Wang H. In-situ formed hierarchical transition metal oxide nanoarrays with rich antisite defects and oxygen vacancies for high-rate energy storage devices. Chin Chem Lett. 2022;33:2669–77.
53. Solymosi F, Rasko J. Thermal decomposition and ignition of ammonium perchlorate in the presence of zinc perchlorate. Z Phys Chem. 1969;67:76–85.
54. Vyazovkin S, Wight CA. Kinetics of thermal decomposition of cubic ammonium perchlorate. Chem Mater. 1999;11:3386–8.
55. Domínguez O. Thermal decomposition of ammonium perchlorate/exfoliated-graphene and the relationship between activation energy and band gap. J Energ Mater. 2019. https://doi.org/10.1080/07370652.2019.1601793.
56. Juibari NM, Eslami A. Synthesis of nickel oxide nanorods by Aloe vera leaf extract: Study of itselectrochemical properties and catalytic effect on the thermal decomposition of ammonium perchlorate. J Therm Anal Calorim. 2019;136:913–23.
57. Garn PD. Temperature coefficient of reaction. Thermochim Acta. 1979;28:185–93.
58. Ninan KN. A thermogravimetric study on the catalytic thermal decomposition of ammonium perchlorate from activation energy normalized through kinetic compensation. Indian J Chem. 1998;37A:295–8.

Authors and Affiliations

Parvathy Chandrababu[1,2] · Sreeja Beena[3] · Deepthi Thomas[1] · Jayalatha Thankarajan[1] · Vishnu Sukumaran Nair[1] · Rajeev Raghavan[1]

✉ Parvathy Chandrababu
c_parvathy@vssc.gov.in

[1] Analytical and Spectroscopy Division, PCM Entity, Vikram Sarabhai Space Centre, Thiruvananthapuram 695022, India

[2] Department of Applied Chemistry, Cochin University of Science and Technology, Cochin, Kerala 682022, India

[3] K.S.M.D.B College, Sasthamcotta, Kollam, Kerala 690521, India